

RSC Applied Polymers

Accepted Manuscript

This article can be cited before page numbers have been issued, to do this please use: B. R. Nelson, V. Scholiers, A. H. Sakamoto, J. F. Rynk, P. A. Pranda, F. E. Du Prez, K. S. Anseth and C. N. Bowman, *RSC Appl. Polym.*, 2026, DOI: 10.1039/D6LP00120C.



This is an Accepted Manuscript, which has been through the Royal Society of Chemistry peer review process and has been accepted for publication.

Accepted Manuscripts are published online shortly after acceptance, before technical editing, formatting and proof reading. Using this free service, authors can make their results available to the community, in citable form, before we publish the edited article. We will replace this Accepted Manuscript with the edited and formatted Advance Article as soon as it is available.

You can find more information about Accepted Manuscripts in the [Information for Authors](#).

Please note that technical editing may introduce minor changes to the text and/or graphics, which may alter content. The journal's standard [Terms & Conditions](#) and the [Ethical guidelines](#) still apply. In no event shall the Royal Society of Chemistry be held responsible for any errors or omissions in this Accepted Manuscript or any consequences arising from the use of any information it contains.

Tailoring Fully Biobased Optical Adhesives via Hydrogen-Bonding Modulation

Benjamin R. Nelson,^{1,2} Vincent Scholiers,^{1,3} Audrey H. Sakamoto,¹ John F. Rynk,⁴ Paula A. Pranda,¹ Filip E. Du Prez,³ Kristi S. Anseth,^{1,2,4} Christopher N. Bowman^{1,4}

Affiliations

¹Department of Chemical and Biological Engineering, University of Colorado Boulder

²BioFrontiers Institute, University of Colorado Boulder

³Polymer Chemistry Research group, Centre of Macromolecular Chemistry (CMaC) and Laboratory of Organic Synthesis, Department of Organic and Macromolecular Chemistry, Faculty of Sciences, Ghent University

⁴Materials Science & Engineering Program, University of Colorado Boulder

Abstract

Display technologies require optical adhesives that simultaneously provide high optical clarity, refractive index control, low birefringence and adhesive strength. However, many commercial adhesive systems rely on petroleum-derived acrylates and isocyanate-based urethanes. Herein, a fully biobased optical adhesive is reported that exploits the initiator-free photopolymerization of dithiolanes. Furthermore, hydrogen bond strength is modulated within the prepared adhesives by changing the chemistry with which the dithiolane is conjugated to a macromolecular core, allowing manipulation of properties including glass transition temperature, adhesion, refractive index, and other optical properties. Throughout these variations, all materials maintain high optical performance, exhibiting visible light transmittance above 98% and haze below 0.7%, coupled with low optical dispersion. These results demonstrate that dithiolanes are readily applied as initiator-free crosslinkers for the formulation of fully biobased optical adhesives.

Introduction

Optical adhesives are crucial components of modern display technologies, where multilayer stacks of functional films are laminated to control the propagation of light through focusing, polarization, brightness enhancement, and diffusion. Interfaces between layers must provide high optical clarity, precise refractive index matching, low birefringence, low dispersion, and robust stability over time. As display architecture becomes both thinner and more flexible, these demands intensify, requiring materials that combine mechanical robustness with finely tuned optical properties, and reduced yellowing over time.¹ Most commonly, optical adhesives rely on a UV-curable (meth)acrylate, often incorporating urethane linkages to improve hydrogen bonding, to transform from a spreadable and wettable liquid during application into a robust solid, interfacial coating after polymerization.^{2, 3} However, utilizing both acrylates and urethanes derived from isocyanates inherently ties optical adhesives to petroleum sources.



The desire to move away from petroleum-based sources has accelerated interest in biobased polymers for high-performance applications.⁴⁻⁷ Among renewable carbon sources, dimers derived from fatty acids are increasingly used, especially in the production of adhesives.⁸⁻¹² Commercially available dimer derivatives, such as Priamine and Pripol, provide long hydrophobic aliphatic backbones with low viscosities and glass transition temperatures, allowing for inherent flexibility. When coupled with photopolymerizable moieties, these cores are advantageous building blocks for the creation of optical adhesive formulations.¹³

1,2-Dithiolanes are an intriguing class of cyclic five-membered disulfide-containing rings that have recently attracted renewed attention and are often derived from naturally occurring resources. Moreover, these functional groups combine several features that make them attractive building blocks for the development of biobased optical materials. For instance, the inherent ring strain of the cyclic disulfide renders them more reactive than their linear counterparts.¹⁴ Since their absorption spectra is red shifted into the visible region, 1,2-dithiolanes undergo photopolymerization without the need for exogenous (and often colored) photoinitiators.^{15, 16} Furthermore, the ring-opening polymerization of 1,2-dithiolanes yields dynamically active (linear) disulfides, which contribute to low birefringence, in part because of reduced shrinkage effects and dynamic bond relaxation, especially when compared to conventional (photo)polymerizations such as (meth)acrylates. Finally, the high sulfur content directly incorporates polarizable sulfur atoms, which contribute to an increased refractive index and enable improved refractive index matching with the substrates to be adhered.¹⁷ Because of these advantages, dithiolanes have found widespread adoption for the creation of dynamic materials.¹⁸⁻²⁰

Despite these advantages, the exploration of dithiolanes as adhesives has been relatively limited. For example, some dithiolane derivatives (e.g., lipoic acid) had been used to create pressure sensitive,²¹⁻²³ structural,^{24, 25} and surgical adhesives; however, many of these reported adhesives are simple linear polymers driven by evaporative or thermal polymerizations.²⁶ More recent formulations have taken advantage of pendant dithiolanes functionalities to enable on-demand photocuring.^{20, 27, 28} Since optical adhesives require transmittance above 95%,²⁹ both the dithiolane concentration and conversion must be managed to allow suitable transmittance, refractive index, and crosslinking density. Balancing effective crosslinking with effective optical performance is essential to realizing the successful development of a fully biobased adhesive system. Additionally, materials applied in optical elements have strict standards regarding yellowing, with photoinitiator fragments often being the source of post-polymerization colored products.³⁰ When coupled with suitable core structures (small molecules with limited crystallinity), no solvent is needed during application, resulting in resins capable of complete incorporation with no extractables at full conversion.

While many dithiolane adhesives have relied on coordination bonding,^{25, 26} supramolecular assembly,³¹ or branching,³² few have investigated the role of hydrogen bonding. In other materials, amide functionalities have primarily been used to increase hydrogen bonding in materials as a strategy to increase T_g and crystallinity.³³ However, urethane linkages remain the dominant



strategy for increasing hydrogen bonding in materials.^{34,35} While the use of urethanes in dithiolane adhesives has only recently been explored,^{27, 36} these studies involved the use of isocyanates to produce urethane bonds. Recently, isocyanate-free synthesis of urethane linkages has emerged as an alternative strategy for incorporating enhanced hydrogen bonding into adhesives without the need for phosgene, as is needed in the classical synthesis of isocyanates.³⁷ This strategy has previously been coupled with bisfunctional amines for the biobased synthesis of isocyanate-free polyurethanes.³⁸ Utilizing a cyclic carbonate, a β -hydroxyurethane can be produced through the reaction with an amine without the need for an isocyanate. For simplicity, this β -hydroxyurethane linkage is referred to as a urethane throughout. Taken together, using esters, urethanes, and amides as coupling chemistries results in a tunable library of hydrogen bonding in adhesives as a method to modulate material properties.

Recently, hydrogen bonding has been increasingly studied in adhesive systems both as an energy dissipation mechanism³⁹ and as a surface adhesion promoter.⁴⁰ These reversible interactions enhance surface contact through specific intermolecular attractions while also acting as sacrificial bonds that break and reform during deformation, increasing energy dissipation and therefore increasing toughness, especially when combined with other dynamic chemistries.³⁹ As a result, hydrogen bonding has been applied to traditional structural adhesives,⁴¹ pressure sensitive adhesives,⁴² surgical adhesives,⁴³ and optical adhesives.⁴⁴ Additionally, hydrogen bonding has seen increased utilization in natural systems that seek to replace petroleum-derived adhesives.⁴⁵ Combined with the photopolymerizability of dithiolanes, tunable hydrogen bonding offers a route to adhesive systems with enhanced bonding and tunable mechanical properties in biobased optical adhesives.

Herein, fully biobased 1,2-dithiolane-derived photocurable crosslinkers are synthesized by functionalizing Priamine and Pripol cores with lipoic acid via ester, amide, and urethane linkages, enabling controlled degrees of hydrogen bonding, all from biobased precursors. Because of the intrinsic ring-strain, these 1,2-dithiolane-based crosslinkers undergo initiator-free photolytic ring-opening polymerization upon UV irradiation over relatively short timescales. The resulting optical adhesives are tunable and exhibit low optical dispersion and high clarity. Their mechanical, adhesive, and optical properties were evaluated and correlated to the extent of hydrogen bonding present in the system. This strategy represents an advancement in the development of sustainable, non-petroleum-derived optical adhesives with excellent clarity and low dispersion. This work establishes a structure-property relationship between hydrogen bond strength and multiple material, adhesive, and optical properties in fully biobased dithiolane crosslinked optical adhesives as a means for showing their overall feasibility in these applications.

Results and Discussion

To synthesize the optical adhesives, the biobased bisfunctional precursors Priamine 1074 and Pripol 2033 were functionalized with lipoic acid, either directly or via incorporation of a glycerol carbonate spacer to form urethane linkages without the need for isocyanates (Figure 1a).



Pripol 2033 was used to prepare ester-linked bisfunctional dithiolanes via Steglich esterification (Figure S1), whereas Priamine 1074 was employed to synthesize both amide-linked (Figure S2) and urethane-linked bisfunctional dithiolanes. For the synthesis of the urethane, the biobased glycerol carbonate was conjugated to lipoic acid with an ester to form lipoic acid glycerol carbonate (LA-GCC, Figure S3), followed by ring-opening of the cyclic carbonate with Priamine, resulting in formation of the urethane (Figure S4). The resulting series provides a library of precursors containing systematic variations in the hydrogen bonding strength, with ester-linked adhesives lacking hydrogen bonding, urethane linkages introducing moderate hydrogen bonding, and amides exhibiting the strongest hydrogen-bonding interactions (Figure 1b).^{46, 47} In addition, a 50:50 mixture of ester- and amide-linked monomers that was photopolymerized into a polymer network (hereafter referred to as mixture) was also investigated as an intermediate hydrogen bonding case, further demonstrating the hydrogen bond strength modulation.

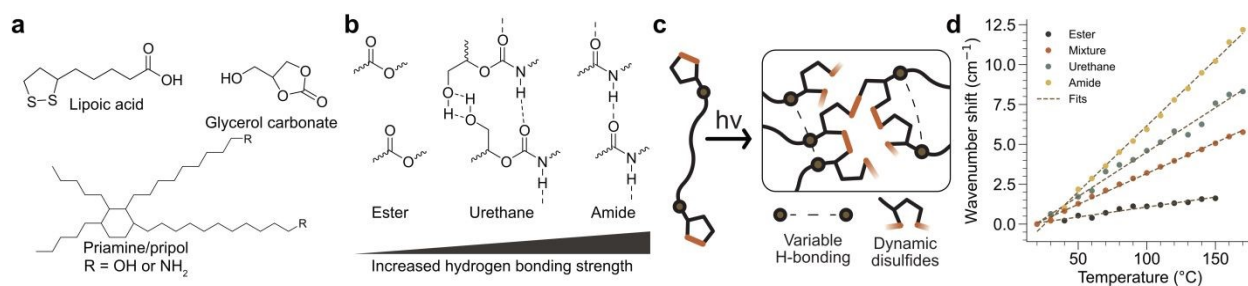


Figure 1. Biobased dithiolane adhesives. (a) Biobased precursors used in the creation of dithiolane adhesives. (b) The hydrogen bond strength increases, moving from the ester to the urethane to the amide linker. (c) Schematic of dithiolane adhesive photocrosslinking, subsequent dynamic disulfide crosslinks, and variable hydrogen bond strength in the adhesive. (d) Centroid location of the C=O stretch during heating in FTIR.

Because of the intrinsic absorption of the dithiolane ring at relevant wavelengths (i.e., 365 nm) (Figure S5), the network precursors are capable of undergoing direct photolytic ring-opening polymerization (Figure 1c). Films were prepared through direct photopolymerization, and the hydrogen bond strength was directly assessed via Fourier transform infrared (FTIR) spectroscopy. Specifically, FTIR of crosslinked samples was used to track the centroid of the C=O stretch over a wide temperature interval, ranging from 20 to 170°C with +10°C intervals (Figure S6). The net displacement of this centroid over the course of the heating program was used as a proxy for hydrogen bond strength, and the slope of this displacement as a function of temperature was used as a quantitative measure of hydrogen bond strength throughout, as has been previously reported (Figure 1d).⁴⁸ The trends observed here confirm the anticipated order of hydrogen bond strength in the materials: ester < mixture < urethane < amide.

To investigate curing behavior, isothermal photorheology was performed by applying a constant small-amplitude oscillatory shear ($T = 25\text{ }^{\circ}\text{C}$, $\gamma = 1\%$, $\omega = 1\text{ rad/s}$) over a defined time period. For this characterization, the sample was first allowed to equilibrate in the darkness for 30 s after which polymerization was initiated by UV irradiation (50 mW/cm² at 365 nm) while simultaneously monitoring and the evolution of the shear storage (G') and loss (G'') moduli



(Figure 2a). All formulations polymerized on relatively short timescales, reaching plateau moduli within 300 s. Taking this reaction rate into account, and to minimize effects of light attenuation, 50 μm adhesive films were produced by exposure to 50 mW/cm^2 of 365 nm light for 2.5 min per side for all subsequent films. Notably, the urethane sample exhibited the slowest polymerization rate and achieved a final plateau modulus lower than the other resins. This behavior might potentially be attributed to the presence of free hydroxyls, resulting from the cyclic carbonate ring-opening. Free hydroxyl functionalities have previously been reported to affect dithiolane polymerization, leading to overall shorter kinetic chains despite similar conversion rates.^{49, 50} Therefore, it is postulated that the urethane sample has shorter dithiolane kinetic chains than the other three samples, leading to a lower crosslinking density and potentially explaining both the slower polymerization and lower storage modulus in the urethane sample.

The influence of variable hydrogen bond strength was further evaluated *via* dynamic mechanical analysis (DMA). In the glassy regime, the storage modulus was found to increase systematically with hydrogen bonding, with the ester sample having the lowest modulus and progressively higher values observed across the series (Figure 2b). This trend was not observed in the rubbery regime, as the hydrogen bonds do not contribute to effective crosslinks in the rubbery modulus at this time scale. Rather, the rubbery storage modulus is virtually the same across the tested samples, except for the urethane, which had a decreased crosslink density. Furthermore, hydrogen bond strength was also found to have a strong effect on the glass transition (T_g) of the samples. As expected, increasing the strength of the hydrogen bonds leads to a systematic increase in the T_g of the samples (Figure 2c).⁵¹ In addition, the breadth of the glass transitions generally increases with additional hydrogen bonding (Figure 2d). However, the urethane sample exhibited an unusually narrow T_g for its location in the hydrogen bonding series. This behavior may result from the same disruption of dithiolane polymerization (shorter kinetic chain lengths) that is speculated to contribute to the decreased rubbery modulus; shorter kinetic chains likely lead to a more homogenous network and therefore a narrower glass transition. These trends in T_g as measured by DMA are recapitulated in differential scanning calorimetry (DSC), again with the same anomaly in the breadth of the urethane T_g (Figure S7).

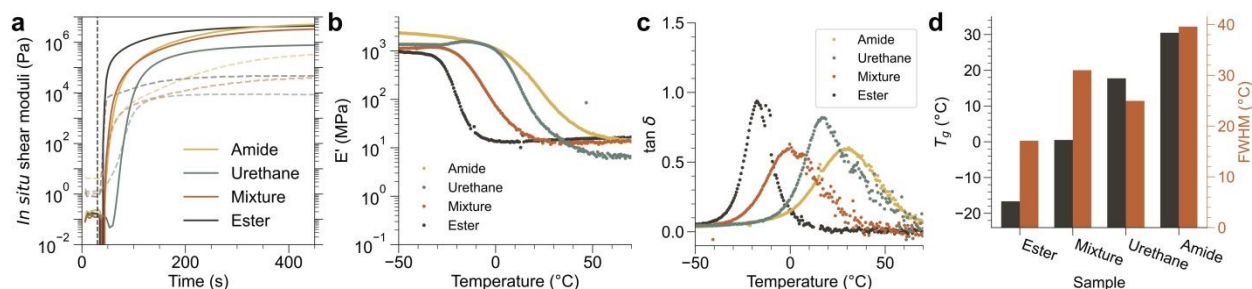


Figure 2. Mechanical properties of dithiolane adhesives. (a) *In situ* photorheology of dithiolane adhesive crosslinking (50 mW/cm^2 , 365 nm, 25 μm thick). (b) E' as a function of temperature in photocrosslinked films. (c) $\tan \delta$ as a function of temperature in photocrosslinked films. (d) Glass transition temperature and FWHM as calculated from the $\tan \delta$ in (c). T_g was additionally measured with dynamic scanning calorimetry in Figure S7. All films polymerized 2.5 min per side, 50 mW/cm^2 at 365 nm, 50 μm thick adhesive.



As solvent resistance is an important characteristic of optical adhesives, the swelling ratio in multiple solvents (toluene, acetone, methanol, and water) was tested for each sample (Figure S8). Unsurprisingly, the swelling ratio trended with hydrogen bond strength, with the amide adhesive having the lowest swelling ratios, being as low as 1.2 in water (Figure S8). In addition, limited extractables are key to adhesive performance. Samples tested via extraction in acetone demonstrated greater than 95% gel fraction (less than 5% extractable) across all formulations (Figure S9). Additionally, flexibility is key for optical adhesives as they are often used to laminate thin films in flexible electronics. These adhesives are highly flexible, as demonstrated through twisting a 50 μm thick amide sample between tweezers (Figure S10). Lastly, while long term stability of materials used as adhesives is important for broad commercial adoption, an evaluation of long term aging is beyond the scope of this work. Generally, dithiolane-crosslinked materials exhibit good stability below temperatures of 120°C, often well above the range of operating temperatures for optical materials outside of specialty applications.⁵²

Next, the adhesive properties of the cured materials were evaluated by lap shear testing using both glass and poly(ethylene terephthalate) as substrates, with three replicate samples tested per condition (Figure 3a). While peel is an important failure mode for optical adhesives, lap shear was chosen as an adhesion metric to correlate with hydrogen bond strength, given that these materials are photocured structural adhesives rather than pressure sensitive adhesives. Transparent substrates were chosen to enable photocuring of the adhesives and due to their relevance in optical applications. Notably, all measurements were taken without applying any adhesion promoters on the substrate surface. While this approach likely leads to a lower ultimate tensile strength, it enables a direct comparison of the effects of the hydrogen bond strength and their interactions with the substrate surface on adhesion. For glass substrates, no clear trend in either the lap shear strength or the strain at break (Figure 3b, Figure S10) was observed. Although intermediate-strength hydrogen bond systems (such as the mixture and urethane) exhibited the highest lap shear strength and strain at break, all samples had large errors associated with the measurements. This error is likely due to interfacial adhesive failures with the substrates, which are more stochastic than cohesive failures, especially in the absence of adhesion promoters.

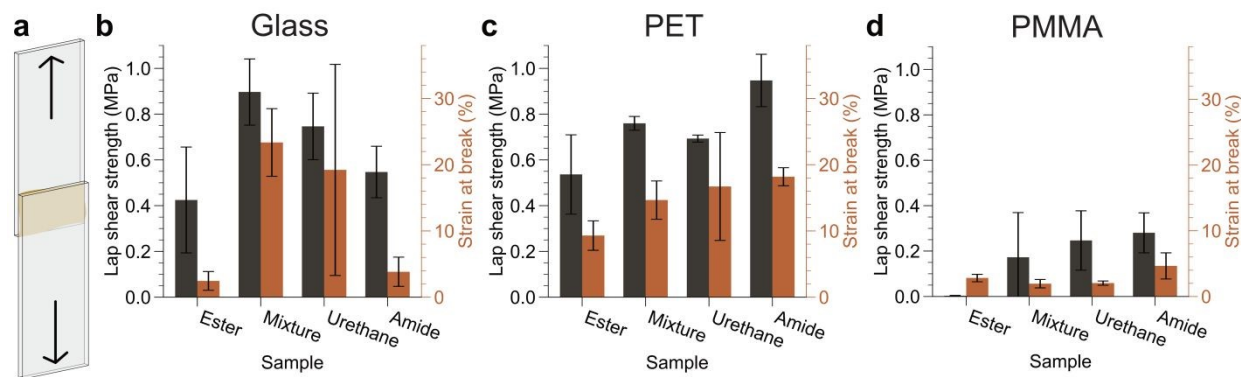


Figure 3. Lap shear adhesive testing of dithiolane adhesives. (a) Schematic of lap shear setup, where two substrates are bonded together at an overlapping joint with adhesive and photocured. (b) Lap shear strength (left axis) and strain



at break (right axis) for samples prepared with a glass substrate. (c) Lap shear strength (left axis) and strain at break (right axis) for samples prepared with a PET substrate. (d) Lap shear strength (left axis) and strain at break (right axis) for samples prepared with a PMMA substrate. All samples polymerized 2.5 min per side, 50 mW/cm² at 365 nm, and 50 μm thick adhesive, with three replicates per condition. Error bars represent standard deviation.

In contrast, for plasma treated PET or PMMA substrates, both lap shear strength and strain at break generally increased with hydrogen bonding strength and had significantly lower variability (Figure 3c-d, Figure S11-12). One potential explanation is the difference in the surface chemistry and roughness. Contact angle measurements with water reveal increased hydrophobicity in both the PMMA and the plasma treated PET as compared to glass (66° on PMMA vs 59° on PET vs 36° on glass, Figure S14), indicating notable differences in surface chemistry and wettability. Compared to the relatively smooth glass microscope slides, the polymeric substrates may facilitate additional mechanical interlocking at the interface. Both factors contribute to PMMA and PET samples having more cohesive failure modes, while the glass had more adhesive failure modes (Figure S15). While these were the predominant modes observed through the lap shear stress-strain curves and sample examination, there is not conclusive evidence to determine that these failure modes are the only ones occurring for all cases.

As previously stated, optical adhesives must meet stringent performance criteria. For instance, high transmittance and low dispersion (high Abbe number) are critical for optically transparent adhesives.¹ All formulations had a high optical clarity, as demonstrated in a transmittance photograph of the amide sample between two glass substrates (Figure 4a). UV-vis spectroscopy, performed on all samples between glass slides after curing, confirmed > 98% transmittance across the visible portion of the spectrum for all samples (Figure 4b), comparable to other optical materials based on sulfur chemistry.⁵³ Additionally, the adhesives exhibited minimal haze, as measured according to the ASTM D1003 standard: All samples measured below 0.3% haze, except for the mixture which had 0.7% haze (Figure S16). Since the one sample that exhibited the higher haze is a mixture of two hydrogen bonding strengths, this increase in haze is potentially attributed to a small extent of micro-phase separation.



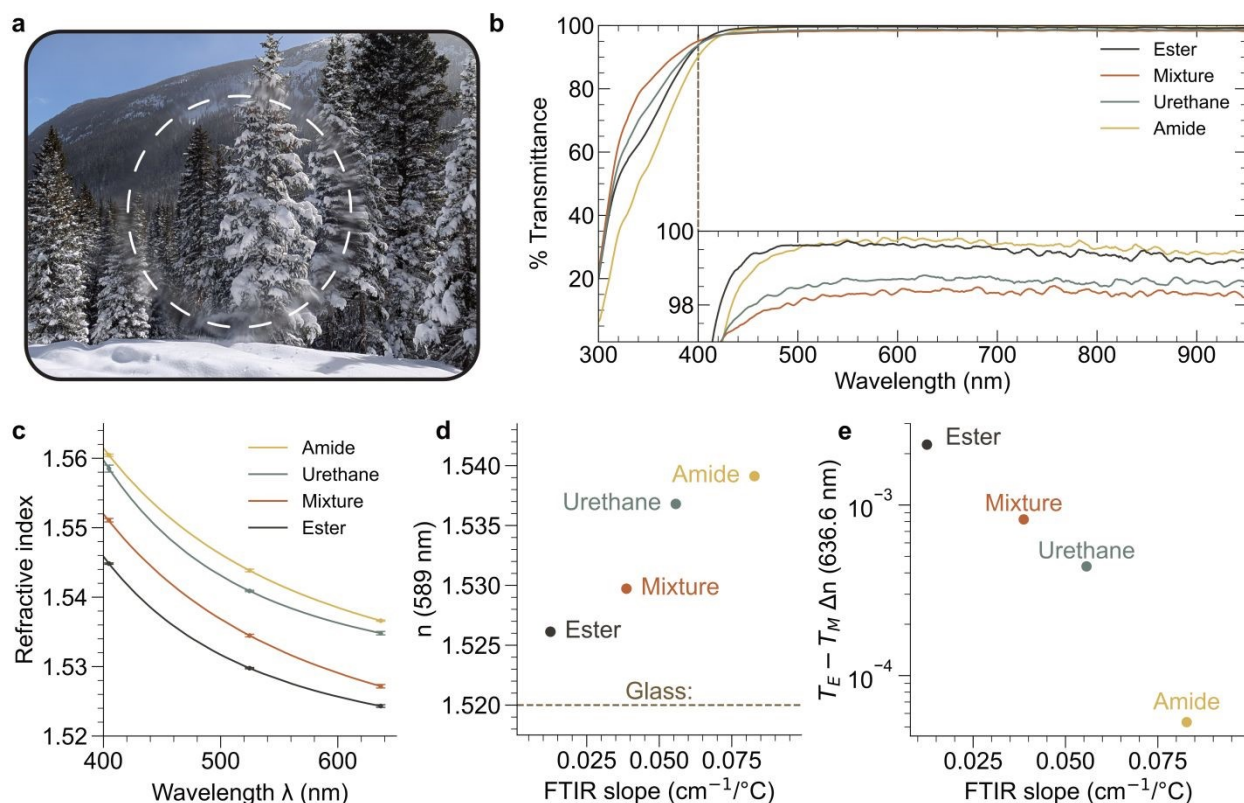


Figure 4. Optical properties of dithiolane adhesives. (a) High transmittance image of a mixture sample between glass substrates. Dashed white line indicates adhesive boundary. (b) Transmittance through each formulation post curing between glass substrates. Inset shows zoomed region between 400 and 950 nm. (c) Refractive index as measured on samples polymerized on PET substrate. Cauchy fit curves of each sample, with the mean and standard deviation of each measured wavelength highlighted (T_E polarization). (d) Refractive index trends with increasing hydrogen bonding as quantified by the slope of the centroid of the C=O stretch as a function of temperature in FTIR (T_E polarization). (e) Birefringence trends with hydrogen bonding (measured at 636.6 nm). All samples polymerized 2.5 min per side, 50 mW/cm^2 at 365 nm, 50 μm thick adhesive.

Refractive index (RI) modulation is another critical property for optical adhesives, as the adhesive must have a relatively close match in refractive index with the substrate to minimize optical aberrations. The RI was measured at 22 $^{\circ}\text{C}$ using a prism coupler refractometer and monochromatic light sources at three wavelengths (λ): 404.7 nm, 524.7 nm and 636.6 nm. Refractometry measures the angular position of total internal reflection. Utilizing PET as the substrate enhanced the substrate and film refractive index difference, minimizing any contributions of the substrate effect. The obtained RI were then fitted to the Cauchy equation (Figure 4c) and used to interpolate the refractive index at the Fraunhofer D line (n_D , $\lambda = 589.3$ nm) for cross-comparison of all formulations. Notably, the refractive index was found to systematically increase with hydrogen bond strength (Figure 4d). This difference is postulated to result from an increased density of the materials as expected from the Lorenz-Lorentz theorem, which correlates the density and polarizability of a material to its refractive index.⁵⁴⁻⁵⁶ However, no clear trend was observed in the Abbe number (V_d), a measure of optical dispersion across wavelengths, which often



decreases with increasing refractive index (Figure S17). Regardless, V_d was comparatively high (representing low optical dispersion) for each of these materials.

Finally, birefringence was evaluated. This optical phenomenon originates from anisotropic effects in the molecular polarizability throughout the material and was quantified by taking the difference in refractive index for light polarized in two orthogonal directions. As many optical applications rely on varied polarizations, minimizing birefringence is of high priority, especially in comparison to commercial urethane-acrylate adhesives where anisotropic shrinkage often leads to stress-laden polymer films with increased birefringence.⁵⁷ To quantify this effect, the RI was quantified in both transverse electric (T_E) and transverse magnetic (T_M) polarization modes, with the difference between these values being the birefringence. At the measurement wavelength of 636.6 nm, increased hydrogen bonding strength results in lower birefringence (Figure 4e). We speculate that increased hydrogen bond strength increases dynamic exchange, enabling further rearrangement after polymerization. Notably, these are all low birefringent materials, with the highest birefringence of 0.002 and the lowest at 0.00005 (below the error of the instrument) compared to many common plastics, such as polycarbonate (0.015), polystyrene (0.019), and even performance acrylates (0.002).⁵⁸ This property is likely due to the ring-opening polymerization of the dithiolanes, which minimizes shrinkage stress during the polymerization, as well as the delayed gelation and disulfide exchange from the polymerization.

Conclusion

In this work, fully biobased dithiolane adhesives with ester, urethane, and amide linkers, were synthesized, creating a library of adhesives with varied hydrogen bond strength. These materials are capable of photopolymerization without the need for exogenous initiator. Hydrogen bond strength was found to have a direct impact on a variety of material properties, including T_g , lap shear strength and strain at break on PET and PMMA substrates, RI, and birefringence. Furthermore, the high optical clarity and tunable refractive indices of these materials makes them well suited to optical adhesive applications. There is a clear structure-property relationship between the hydrogen bond strength and multiple material, adhesive and optical properties, establishing tunability of properties through hydrogen bond strength in these dithiolane-crosslinked, fully biobased optical adhesives.

Acknowledgements

The authors gratefully acknowledge funding from the Industry University Cooperative Research Center for Fundamentals and Applications of Photopolymerizations (C. N. B. and B. R. N), and the National Heart, Lung, and Blood Institute (NHLBI, Grant number: R01 HL171197, K.S.A.). V.S and F.D.P. would like to thank the Research Foundation Flanders (FWO) (Application 1S34725N and V410425N) for financial support. FEDP acknowledges BOF-UGent



for GOA funding (BOF21/GOA/007). The authors would like to thank B. E. Kirkpatrick and J. Debuyck for their fruitful discussions, and S. A. Klug for experimental assistance.

References

1. Y. Du, Y. Li, C. Li, R. Xu, L. Meng and Y. Bai, *ACS Applied Materials and Interfaces*, 2025, 17, 5578-5594.
2. W. Ming, Z. Xie, Z. Jiang, Y. Chen, G. Zhang, Y. Xu and W. He, *Journal of the Society for Information Display*, 2022, 30, 851-876.
3. G. Wang, Z. Zhou, M. Chen, J. Wang and Y. Yu, *ACS Applied Polymer Materials*, 2023, 5, 2051-2061.
4. Y. Liu, M. L. Wu, Y. D. Li, L. Y. Li and J. B. Zeng, *ACS Sustainable Chemistry & Engineering*, 2023, 11, 17190-17198.
5. L. Pezzana, G. Melilli, P. Delliere, D. Moraru, N. Guigo, N. Sbirrazzuoli and M. Sangermano, *Progress in Organic Coatings*, 2022, 173.
6. J. A. McLaughlin, E. Kinaci and G. R. Palmese, *ACS Applied Polymer Materials*, 2024, 6, 11733-11742.
7. L. Pezzana and M. Sangermano, *Progress in Organic Coatings*, 2021, 157, 106295.
8. F. Van Lijsebetten, T. Maiheu, J. M. Winne and F. E. Du Prez, *Advanced Materials*, 2023, 35, e2300802.
9. S. Liang, H. Zhao, X. Li, Y. Feng and J. Zhao, *ACS Applied Polymer Materials*, 2024, 6, 9615-9626.
10. P. Ranganathan, C.-W. Chen, M.-C. Tasi, S.-P. Rwei and Y.-H. Lee, *Industrial & Engineering Chemistry Research*, 2021, 60, 12139-12154.
11. C. R. Frihart, *Polymers (Basel)*, 2023, 15.
12. R. F. R. Freitas, C. Klein, M. P. Pereira, R. B. Duczinski, S. Einloft, M. Seferin and R. Ligabue, *Journal of Adhesion Science and Technology*, 2015, 29, 1860-1872.
13. J. Liu, K. Wang, Y. Xie, F. Gao, Q. Zeng, Y. Yuan, R. Liu and X. Liu, *Journal of Coatings Technology and Research*, 2017, 14, 1325-1334.
14. L. J. Reed, B. G. Debusk, I. C. Gunsalus and G. H. F. Schnakenberg, *Journal of the American Chemical Society*, 1951, 73, 5920-5920.
15. J. A. Barltrop, P. M. Hayes and M. Calvin, *Journal of the American Chemical Society*, 1954, 76, 4348-4367.
16. R. B. Whitney and M. Calvin, *Journal of Chemical Physics*, 1955, 23, 1750-1756.
17. S. P. Keyser, M. Trujillo-Lemon, A. N. Sias, B. D. Fairbanks, R. R. McLeod and C. N. Bowman, *ACS Applied Materials and Interfaces*, 2024, 16, 45577-45588.
18. C. Choi, J. L. Self, Y. Okayama, A. E. Levi, M. Gerst, J. C. Speros, C. J. Hawker, J. Read de Alaniz and C. M. Bates, *Journal of the American Chemical Society*, 2021, 143, 9866-9871.
19. Q. Zhang, Y. X. Deng, H. X. Luo, C. Y. Shi, G. M. Geise, B. L. Feringa, H. Tian and D. H. Qu, *Journal of the American Chemical Society*, 2019, 141, 12804-12814.
20. B. Sieredzinska, Q. Zhang, K. Berg, J. Flapper and B. L. Feringa, *Chemical Communications*, 2021, 57, 9838-9841.
21. K. R. Albanese, Y. Okayama, P. T. Morris, M. Gerst, R. Gupta, J. C. Speros, C. J. Hawker, C. Choi, J. R. de Alaniz and C. M. Bates, *ACS Macro Letters*, 2023, 12, 787-793.



22. K. V. Dikshit, A. M. Visal, F. Janssen, A. Larsen and C. J. Bruns, *ACS Applied Materials and Interfaces*, 2023, 15, 17256-17267.
23. S. Luo, N. Wang, Y. Pan, B. Zheng, F. Li and S. Dong, *Small*, 2024, 20, e2310839.
24. Y. Deng, Q. Zhang, C. Shi, R. Toyoda, D. H. Qu, H. Tian and B. L. Feringa, *Science Advances*, 2022, 8, eabk3286.
25. Q. Zhang, C. Y. Shi, D. H. Qu, Y. T. Long, B. L. Feringa and H. Tian, *Science Advances*, 2018, 4, eaat8192.
26. S. Pal, J. Shin, K. DeFrates, M. Arslan, K. Dale, H. Chen, D. Ramirez and P. B. Messersmith, *Science*, 2024, 385, 877-883.
27. Z. Q. Liu, C. Z. Ju, P. L. Li, Z. C. Yan and Z. Zhang, *Journal of Applied Polymer Science*, 2025, 142.
28. S. Maes, V. Scholiers and F. E. Du Prez, *Macromolecular Chemistry and Physics*, 2022, 224, 2100445.
29. S.-W. Lee, J.-W. Park, C.-H. Park, Y.-E. Kwon, H.-J. Kim, E.-A. Kim, H.-S. Woo, S. Schwartz, M. Rafailovich and J. Sokolov, *International Journal of Adhesion and Adhesives*, 2013, 44, 200-208.
30. J. Seguro, N. S. Allen, M. Edge, A. McMahon and S. Wilson, *Polymer Degradation and Stability*, 1999, 64, 39-48.
31. H. Y. Lin, L. Li, Q. Zhang, D. H. Qu and F. Tong, *Chemistry*, 2025, 31, e202500900.
32. S. Pal, E. E. Salzman, D. Ramirez, H. Chen, C. A. Perez, K. Dale, S. K. Ghosh, L. Lin and P. B. Messersmith, *Journal of the American Chemical Society*, 2025, 147, 13377-13384.
33. C. J. Reese, G. M. Musgrave, P. Cardon, H. Ji, M. Shusteff and C. Wang, *ACS Macro Letters*, 2025, 14, 1189-1194.
34. D. K. Chattopadhyay and K. V. S. N. Raju, *Progress in Polymer Science*, 2007, 32, 352-418.
35. V. Scholiers, B. Hendriks, S. Maes, T. Debsharma, J. M. Winne and F. E. Du Prez, *Macromolecules*, 2023, 56, 9559-9569.
36. Y. J. Zhou, N. N. Xia, J. L. Zhang, T. X. Li, J. M. Wang and Q. Wu, *ACS Sustainable Chemistry & Engineering*, 2025, 13, 6412-6422.
37. L. Maisonneuve, O. Lamarzelle, E. Rix, E. Grau and H. Cramail, *Chemical Reviews*, 2015, 115, 12407-12439.
38. K. Błażek, P. Kasprzyk and J. Datta, *Polymer*, 2020, 205.
39. S. Chen, K. Zhang, Z. Li, Y. Wu, B. Zhu and J. Zhu, *Supramolecular Materials*, 2023, 2.
40. K. Viswanathan, H. Ozhalici, C. L. Elkins, C. Heisey, T. C. Ward and T. E. Long, *Langmuir*, 2006, 22, 1099-1105.
41. W. Xiang and J. Xia, *ACS Omega*, 2024, 9, 13644-13654.
42. M. M. Feldstein, E. E. Dormidontova and A. R. Khokhlov, *Progress in Polymer Science*, 2015, 42, 79-153.
43. Q. Zhang, Z.-Y. Xu and W.-G. Liu, *Chinese Journal of Polymer Science*, 2024, 42, 1619-1641.
44. C. Lin, B. Qin and J. Xia, *ACS Applied Polymer Materials*, 2025, 7, 10686-10700.
45. S. Wu, C. Cai, F. Li, Z. Tan and S. Dong, *CCS Chemistry*, 2021, 3, 1690-1700.
46. J.-Y. Le Questel, C. Laurence, A. Lachkar, M. Helbert and M. Berthelot, *Journal of the Chemical Society, Perkin Transactions 2*, 1992, 12, 2091-2094.



47. C. B. Berlin, E. Sharma and M. C. Kozlowski, *The Journal of Organic Chemistry*, 2024, 89, 4684-4690.
48. M. T. Lemon, M. S. Jones and J. W. Stansbury, *Journal of Biomedical Materials Research Part A*, 2007, 83, 734-746.
49. P. R. Brown and J. O. Edwards, *The Journal of Organic Chemistry*, 1969, 34, 3131-3135.
50. P. R. Brown and J. O. Edwards, *Journal of Chromatography*, 1969, 43, 515-518.
51. T. K. Kwei, *Journal of Polymer Science: Polymer Letters Edition*, 1984, 22, 307-313.
52. Q. Zhang, B. L. Feringa, D. H. Qu and H. Tian, *Accounts of Chemical Research*, 2026, 59, 151-164.
53. S. S. Chen, V. Scholiers, H. Chen, X. W. An, J. J. Li, J. Zhu, F. E. Du Prez and X. Q. Pan, *Chinese Journal of Polymer Science*, 2025, 43, 2022-2029.
54. S. Watanabe, T. Takayama and K. Oyaizu, *ACS Polymers Au*, 2022, 2, 458-466.
55. B. Yuan, L. Tian, J. Bai, Y. Zhang, Y. Peng, J. Cui, Z. Fan, M. Guo, Y. Li and B. Cheng, *Polymer*, 2026, 348.
56. B. F. Hanley, *Materials Today Communications*, 2020, 25.
57. Y. Jeon, J. Choi, D. Seo, S. H. Jung and J. Lim, *Polymer Chemistry*, 2023, 14, 1117-1123.
58. Y. Tojo, Y. Arakawa, J. Watanabe and G.-i. Konishi, *Polymer Chemistry*, 2013, 4.



All data needed to evaluate the conclusions in the paper are present in the paper and/or the ESI. Raw data are available from the authors upon reasonable request.

